Supplemental Material Contents

- Supplemental Information A: Operating Parameters for AM Serial Flow Cytometry
- Supplemental Information B: Optimization for Noise Threshold Finding
- Supplemental Information C: Subpopulation Grouping
- Supplemental Information D: Overlaps
- Supplemental Information E: Power Attenuation at Fiber Combiner
- Supplemental Information F: Data

Supplemental Information A: Operating Parameters for AM Serial Cytometry

Table S1: Some operating parameters utilized by the AM serial flow cytometer in this study.

Parameter	Var	Base or Derived	This study	Equation or Constraints
Measurement region	L, W, H	Base	132 µm × 40 µm × 80 µm	-
Particle concentration in particles/mL	C	Base	1 x 10^6 particles mL^{-1}	-
Flow rate in mL/s	Q	Base	37 µL min^{-1}	$Q < 100$
Particle passage rate	P	Derived	24 particles s^{-1}	$C \cdot Q$
Duration of pulse	D	Derived	620 µs	L ÷ Q / (W x H)
Photodetector characteristic frequency	-	Base	1.8 x 10^9 s^{-1}	-
DAQ frequency	f_{DAQ}	Base	2 x 10^6 samples s^{-1}	-
Data sampling window width	W	Base	5000 samples	-
FFT bin width	B	Derived	Intervals of 400 s^{-1}	f_{DAQ} ÷ W
AM frequencies	f_{c1}, f_{c2}	Base	125 200 cycles s^{-1} and 200 000 cycles s^{-1}	$< f_{DAQ} \div 10 \frac{\text{samples}}{\text{cycle}}$, = multiple of B
AM oscillations per pulse	f_{rel}	Derived	80 cycles per pulse to 120 cycles per pulse	$D \div \frac{1}{f_c} > 30 \frac{\text{cycles}}{\text{pulse}}$
Photodetector gains	V_G	Base	Generally 800 mV to 1000 mV	$600\ \text{mV} < V_G$, $V_G < 1050\ \text{mV}$

Supplemental Information B: Optimization for Noise Threshold Finding

We separated the top five brightest microsphere subpopulations from the noise, for both region 1 and region 2 on the combined AM channel, by plotting a histogram of the fluorescence FFT peak amplitudes and graphically finding the threshold value (data not shown). Then, because the threshold was so close to both the noise and the fifth brightest subpopulation in the combined AM channel, a threshold optimization was performed. As shown in Figure S1, the noise thresholds for combined AM channel region 1 and region 2 varied by intervals of 10 % between 70 % and 130 % of the initial estimate (i.e., 100 %), with intervals of 2.5 % on the inner +/- 10 % (dashed black lines). At each of these possible thresholds, the complete data analysis of the 3755-pulse dataset was performed, from raw data aggregation through region decoding and matching and yield counting. The accuracy of decoding the fifth-brightest microsphere subpopulation (solid blue line) showed a rise as the threshold varied from 70 % to around 97.5 %, where the accuracy value plateaued with accuracy near 100 %. The matching yield also rose as the threshold increased from 70 % to 102.5 %, where it peaked with a yield of 97.6 % before dropping slightly for higher thresholds (dashed blue line). Also shown is the pulse count in the fifth-brightest microsphere subpopulation, which includes spurious noise pulses when the threshold is too low and missed relevant microsphere passage pulses when the threshold is too high (orange line). Between these extremes, there is a relatively level zone where the derivative of the pulse count with the threshold is low, which corresponds with the peak in the matching yield percent. Per these results, the selected threshold was therefore set at 102.5 %, the visually estimated threshold value, and is marked with a dot-and-dashed red line. Within 5 % of the selected threshold, the detection count, decoding accuracy, and matching yield varied by less than 5 %, 1% and 1 %, respectively. This selected threshold was used as the noise threshold for all the data presented in this paper.

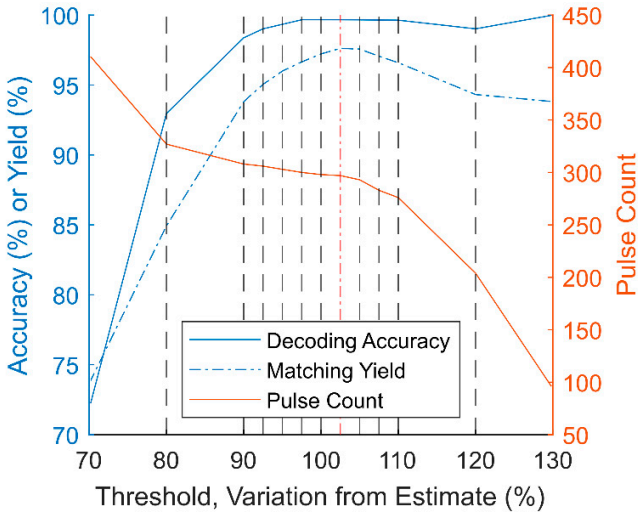


Figure S1: Optimization of noise threshold value, as a variation in percent from an operator-selected estimate of the noise threshold (100 %). The iterated threshold variation values are shown with dashed black lines. Decoding accuracy of the fifth-brightest microsphere subpopulation, overall matching yield, and pulse count of the fifth-brightest microsphere subpopulation are shown as functions of the noise threshold. The peak matching yield occurs at the threshold iteration shown with a dot-and-dashed red line.

Supplemental Information C: Subpopulation Grouping

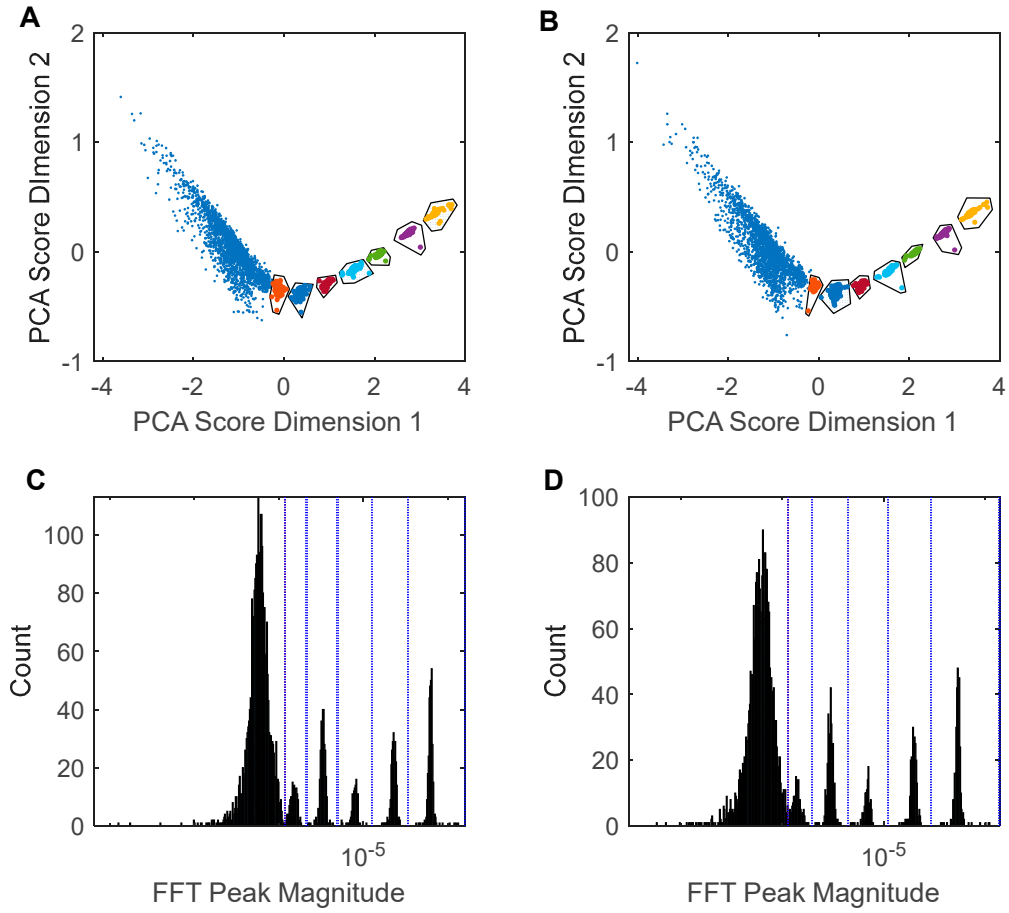


Figure S2: Subpopulation grouping. (A) Region 1 ground truth subpopulation grouping, as gated on a 2-dimensional principal component analysis (PCA) generated from area, width, and height measurements of pulses. The streak of unselected pulses is a combination of dim pulses and noise. (B) Region 2 ground truth subpopulation grouping, generated in the same manner as Region 1. (C) Region 1 AM subpopulation grouping, as gated on a histogram generated from the FFT peak magnitudes at the R1 carrier frequency. The peak left of the purple line is a combination of dim pulses and noise. (D) Region 2 AM subpopulation grouping, generated in the same manner as Region 1.

Supplemental Information D: Overlaps

Estimating Likelihood of Coincident Event

The probability of k microspheres existing in a region simultaneously can be estimated as the output of a Poisson distribution function, with the λ parameter (expected number of pulses) calculated as the product of microsphere concentration C and measurement volume V, as shown in Equation S1 and Table S2. The condition where two (or more) microspheres exist in a single measurement region simultaneously is referred to as a doublet (or multiplet). The probability of doublets and multiplets occurring is denoted Pr(2+) and contributes negligibly to the probability of an overlap. The probability of an overlap having occurred during any given pulse detection in a 2-region cytometer is $\mathrm{Pr}_2(\,2 \mid 1+)$. With these definitions, a model of the probability of overlapping pulses from multiple regions in a 2-region cytometer is described in Equations S2 and S3.

$$\mathrm{Pr}(k) = \frac{\boldsymbol{\lambda}^k \boldsymbol{e}^{-\lambda}}{k!}, \text{ where } \boldsymbol{\lambda} = C \cdot V$$

Equation S1: The Poisson distribution gives the probability of k microspheres existing simultaneously in a measurement region.

Table S2: Probabilities of single-region microsphere counts as a function of sample concentration.

Probability of Number of Microspheres	**Concentration:**		
	500 000 microspheres/mL	**1 000 000 microspheres/mL**	**2 000 000 microspheres/mL**
Pr(0)	99.26 %	98.53 %	97.09 %
Pr(1)	0.73 %	1.46 %	2.87 %
Pr(2)	0.00003 %	0.0001 %	0.0004 %
…	negligible		

$$\mathrm{Pr_n}(k) \rightarrow \mathrm{Pr}_2(k) = \ {}_2C_k \cdot \mathrm{Pr}(0)^{2-k} \cdot \mathrm{Pr}(1)^k$$

Equation S2: A model where n is the number of regions in the chip (i.e., 2) and k is the number of detected pulses, with terms for the probability of zero microspheres per region and one microsphere per region, and which gives the probability of pulses in k regions occurring at a time (i.e., an overlap if $k \geq 2$), for the case of $n = 2$ regions in the chip.

$$\mathrm{Pr}_2\ (\,2 \mid 1+) = \frac{1 - \mathrm{Pr}_2(0) - \mathrm{Pr}_2(1)}{1 - \mathrm{Pr}_2(0)}$$

Equation S3: Chance of an overlap occurring in a 2-region chip in terms of probabilities of 0 or 1 pulses occurring at a time.

For a population concentration of 1 000 000 microspheres per mL, Equation 3 gives the probability of 1.47 % overlaps in detected pulses for a 2-region cytometer of our design. For similar cytometers with greater numbers of regions, probabilities are shown in Table S3. These compare with an experimental 2-region dataset with $N = 3755$ detected signal pulses, in which 1.23 % of pulses were overlapped signals.

Table S3: Probabilities of overlapping pulses occurring for AM cytometers with 2, 3, and 4 detection regions. Concentration: 1 M particles per mL

Region Count	$\mathbf{Pr_n(2+ \mid 1+)}$
$\boldsymbol{n = 2}$	1.47 %
$\boldsymbol{n = 3}$	2.20 %
$\boldsymbol{n = 4}$	2.93 %

Supplemental Information E: Power Attenuation at Fiber Combiner

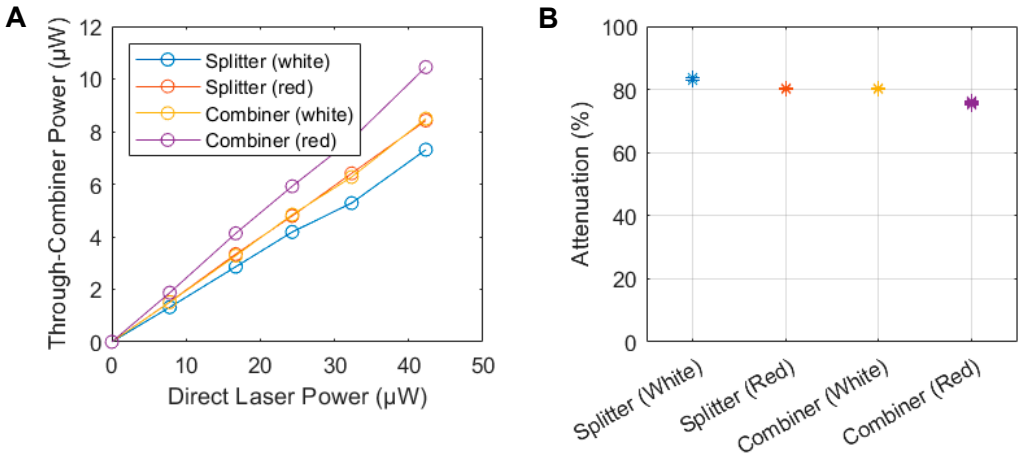


Figure S3: Power attenuation at fiber combiner. The fiber combiner was a commercially available 2-to-1 union of optical fibers that could be connected in either direction, i.e., as a combiner or a splitter. The split end of the combiner/splitter consisted of two optical fibers, one white and one red. (**a**) Direct laser power was measured by an optical power meter with laser light passing through a patch cable. The combiner/splitter was then connected to the laser source in place of the patch cable. Power output through the combiner/splitter was measured by the optical power meter. This process was performed five times per direction and color, to collect a series of through-combiner power measurements at a range of laser power levels. (**b**) The data in panel A was used to calculate an attenuation percentage for each power level and for each direction and fiber color, presented in panel B as asterisks, where each set of five data points are nearly coincident. The data suggest that within the range tested, the attenuation percentage was independent of laser power.

Supplemental Information F: Data

The provided Excel spreadsheet file contains data from each pulse of the 3755 in the dataset reported in this publication. Every row corresponds to a pulse, and columns are annotated as follows.

Column	Variable Name	Variable Description	Unit
A	Time	Pulse time	s
B	RFB_GT1	ground truth pulse relative fluorescence brightness (area) *calculated as integrated area under the curve of the pulse waveform	V · s
C	RFB_GT2	ground truth pulse relative fluorescence brightness (area) *calculated as integrated area under the curve of the pulse waveform	V · s
D	RFB_CR	combined-region pulse relative fluorescence brightness (area) *calculated as the first-mode amplitude, equal to the area under the curve of the pulse waveform	V · s
E	RFB_CR_FFT_R1	combined-region pulse relative fluorescence brightness (FFT peak amplitude) *calculated as the FFT peak amplitude at the frequency of region 1 (125 200 cycles/s)	V
F	RFB_CR_FFT_R2	combined-region pulse relative fluorescence brightness (FFT peak amplitude) *calculated as the FFT peak amplitude at the frequency of region 2 (200 000 cycles/s)	V
G	detection_description_R1	detection description, region 1 (1: no CR detection, 2: missing CR detection, 3: spurious CR detection, 4: positive CR detection)	N/A
H	detection_description_R2	detection description, region 2 (1: no CR detection, 2: missing CR detection, 3: spurious CR detection, 4: positive CR detection)	N/A
I	class_GT	classification by ground truth, down to 5th brightest bead (1: no detection, 2: detection in region 1, 3: detection in region 2, 4: detection in both regions)	N/A
J	class_GT_7	classification by ground truth, down to 7th brightest bead (1: no detection, 2: detection in region 1, 3: detection in region 2, 4: detection in both regions)	N/A
K	class-CR	classification by combined region, down to 5th brightest bead (1: no detection, 2: detection in region 1, 3: detection in region 2, 4: detection in both regions)	N/A
L	subpopulation_GT_R1	subpopulation identified by ground truth, for region 1 (from 1 through 8, 1 = brightest bead, 7 = 7th brightest bead, 8 = indistinguishable from noise)	N/A
M	subpopulation_GT_R2	subpopulation identified by ground truth, for region 2 (from 1 through 8, 1 = brightest bead, 7 = 7th brightest bead, 8 = indistinguishable from noise)	N/A
N	subpopulation_CR_R1	subpopulation identified by combined region, for region 1 (from 1 through 6, 1 = brightest bead, 5 = 5th brightest bead, 6 = indistinguishable from noise)	N/A
O	subpopulation_CR_R2	subpopulation identified by combined region, for region 2 (from 1 through 6, 1 = brightest bead, 5 = 5th brightest bead, 6 = indistinguishable from noise)	N/A
P	serialized_index_GT_R1	serialized index by ground truth, for region 1. Index refers to count of matched pulses, corresponding to pulses from microspheres passing region 1 and later region 2. NaN implies the pulse was not matched	N/A
Q	serialized_index_GT_R2	serialized index by ground truth, for region 2. Index refers to count of matched pulses, corresponding to pulses from microspheres passing region 1 and later region 2. NaN implies the pulse was not matched	N/A
R	serialized_index_CR_R1	serialized index by combined region, for region 1. Index refers to count of matched pulses, corresponding to pulses from microspheres passing region 1 and later region 2. NaN implies the pulse was not matched	N/A
S	serialized_index_CR_R2	serialized index by combined region, for region 2. Index refers to count of matched pulses, corresponding to pulses from microspheres passing region 1 and later region 2. NaN implies the pulse was not matched	N/A

Abbreviations: RFB: relative fluorescence brightness, GT: ground truth, CR: combined region, FFT: fast Fourier transform, R1: region 1, and R2: region 2.